CASE REPORT

Microvascular dysfunction and cardiac fibrosis in heart failure with preserved ejection fraction: a case report

Nikhil Narang[1], Diego Medvedofsky[1], Kathryn Dryer[2], Sanjiv J. Shah[3], Charles J. Davidson, Amit R. Patel[1] and John E.A. Blair[1]*

[1]*Section of Cardiology, Department of Medicine, University of Chicago, Chicago, IL 60637, USA;* [2]*Pritzker School of Medicine, University of Chicago, Chicago, IL 60637, USA;* [3]*Division of Cardiology, Department of Medicine, Northwestern University Feinberg School of Medicine, Chicago, IL 60611, USA*

Abstract

We report the case of a 55-year-old woman with heart failure with preserved ejection fraction (HFpEF), who presented with hypertensive urgency and pulmonary oedema. The patient was medically optimized and underwent cardiac catheterization revealing pulmonary hypertension, elevated pulmonary capillary wedge pressure, normal cardiac index, and non-obstructive coronary disease. Invasive evaluation of coronary flow revealed blunted coronary flow reserve and increased index of microvascular resistance. Cardiac magnetic resonance imaging demonstrated reduced global myocardial perfusion and diffuse interstitial fibrosis. This case exhibits a potential HFpEF phenotype associated with microvascular dysfunction, fibrosis, and elevated filling pressures.

Introduction

Heart failure with preserved ejection fraction (HFpEF) is a growing epidemic that confers a rate of hospitalization and mortality approaching that of heart failure with reduced ejection fraction (HFrEF).[1] An emerging pathophysiological model of HFpEF is based on the concept that underlying pre-existing conditions associated with HFpEF lead to coronary microvascular and endothelial inflammation, increased oxidative stress, and depletion of nitric oxide-cyclic guanosine monophosphate protein kinase-G signalling, which promotes myocardial fibrosis.[2] This case demonstrates the pathophysiology of HFpEF phenotype through invasive and non-invasive diagnostic modalities.

Case report

A 55-year-old woman with a history of chronic obstructive pulmonary disease, hypertension, and type 2 diabetes presented with four days of dyspnoea and chest pressure.

Blood pressure was 220/100 mmHg, respirations 40 per minute, oxygen saturation of 84% on room air, and a heart rate of 125 beats per minute. She had a rapid regular rhythm, S3 gallop prior to S1 and S2 heart sounds. Pulmonary exam revealed bilateral inspiratory crackles. Extremities were without oedema.

Serum renal and liver function tests were within normal limits, and N-terminal pro-B-type natriuretic peptide was 1957 pg/mL (normal <125 pg/mL). She was placed on non-invasive positive pressure ventilation, intravenous nitroglycerine and furosemide drips and transferred to the cardiac intensive care unit. Electrocardiogram showed sinus tachycardia with left ventricular hypertrophy (LVH). Chest radiography showed cardiomegaly and bilateral opacities consistent with pulmonary oedema. Transthoracic echocardiography demonstrated concentric LVH, left ventricular ejection fraction (LVEF) of 70%, restrictive filling pattern on mitral inflows, severely enlarged left atrium, and normal right ventricular function.

After stabilization, she underwent coronary angiography and right heart catheterization. She had elevated pulmonary pressures (systolic/diastolic/mean: 62/21/39 mmHg) and

pulmonary capillary wedge pressure (28 mmHg), with preserved cardiac output and index by thermodilution (5.7 L/min and 3.5 L/min/m^2, respectively). Coronary angiography revealed non-obstructive coronary disease with an elevated left ventricular end-diastolic pressure of 30 mmHg. A coronary physiology study was performed. Following systemic heparinization, a 6-French Extra Back-Up 3.5 guiding catheter was advanced into the left main coronary artery, and a 0.014-inch coronary flow wire (Certus, St. Jude Medical®) was placed in the distal 2/3 of the left anterior descending artery after pressure calibrations. After the 200 μg of nitroglycerine was administered, three coronary thermodilutions were performed using 3 mL room temperature saline boluses administered through the guiding catheter. Mean transit time (T_m) was measured before (0.70 s) and after (0.44 s) induction of hyperaemia using 140 μg/kg/min adenosine drip administered centrally. Distal coronary and catheter pressure measurements were also measured (56 and 63 mmHg, respectively). Fractional flow reserve (distal/proximal coronary pressure at hyperaemia) was 0.87, coronary flow reserve (CFR, $T_{m\text{-resting}}/T_{m\text{-hyperaemia}}$) 1.6, and index of microvascular resistance (IMR, T_m × distal coronary pressure at hyperaemia) 24.5 units, consistent with inadequate coronary flow reserve and elevated microvascular resistance (*Figure 1*, Panel A).

Figure 1 (A) Coronary physiology tracing with thermodilution curves. T_m at baseline was 0.70 ms (white arrow) and 0.44 ms during hyperaemia (orange arrow) resulting in a coronary flow reserve (CFR) of 1.6 and an index of microvascular resistance (IMR) of 24, consistent with microvascular dysfunction. (B) Late gadolinium enhancement images are shown in the two-chamber and three-chamber views, respectively. There is a subtle region of late gadolinium enhancement noted in the basal inferior and inferolateral wall (white arrows). The pattern is atypical for prior myocardial infarction and suggests the presence of underlying myocardial fibrosis, inflammation, or infiltration. (C) Stress perfusion images are shown in short-axis views at three different levels of the left ventricle. No perfusion defects were present during hyperaemia; however, myocardial perfusion reserve index calculated as the ratios of stress to resting signal uptake slope normalized to stress and resting left ventricular (LV) cavity uptake slope and found to be 0.33 (normal 1.78 ± 0.60), suggesting microvascular dysfunction. (D) Native T_1-weighted mapping of basal, mid, and apical short axis. The native myocardial T_1-weighted relaxation time is 1203 ms, which is significantly elevated. Pre-contrast and post-contrast images from a modified Look-Locker imaging T_1-weighted mapping pulse sequence are shown along with the representative relaxation curves for the LV septal myocardium and LV cavity. These curves were used to calculate the extracellular volume fraction (ECV), by multiplying 1-hematocrit by Δ1/T_1 of myocardium normalized to Δ1/T_1 of blood and found to be 36.4% (normal 20–30%). Both of these findings support the presence of an underlying fibrosing, infiltrative, or inflammatory process. FFR, fractional flow reserve.
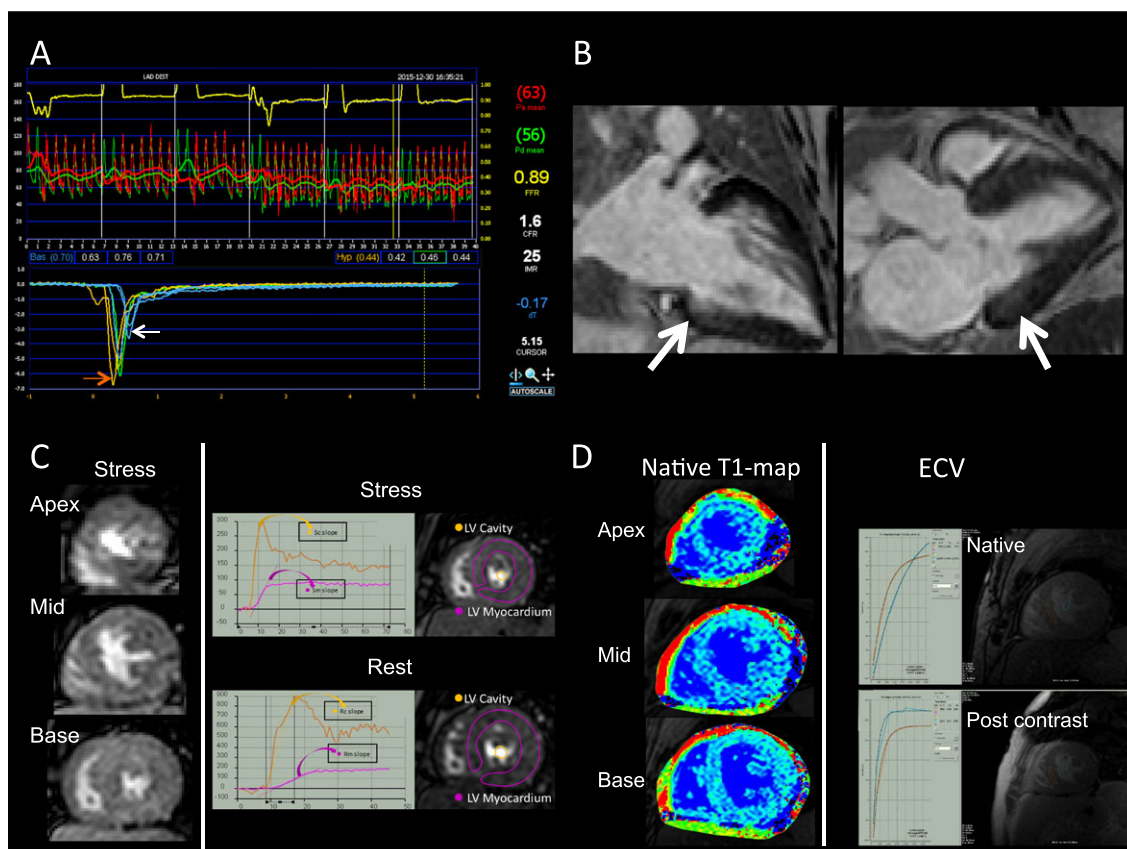
Cardiac magnetic resonance imaging (CMR) vasodilator study with and without contrast was performed. Hyperaemia was induced with regadenoson 0.4 mg intravenous, and within 1 min 0.1 mmol/kg Gd-DTPA was infused at 4 mL/s and left ventricular (LV) myocardial and cavity signal intensity over time was measured at hyperaemia, and repeated following reversal of hyperaemia with aminophylline. Resting CMR cine-sequences demonstrated LV end-diastolic volume index 97 mL/m^2, LVEF 67%, and a small region of late gadolinium enhancement (LGE) in the basal inferior and inferolateral wall (*Figure 1*, Panel B). Myocardial perfusion reserve index (MPRi), calculated as the ratios of stress to resting signal uptake slope, normalized to stress and resting LV cavity uptake slope, was 0.33—below that of healthy outpatients in our institution of 1.78 ± 0.60 (*Figure 1*, Panel C). Extracellular volume fraction (ECV) was calculated using T_1-weighted spin-echo and a modified Look-Locker inversion recovery sequence before and 15 min after contrast by multiplying 1-haematocrit by $\Delta 1/T_1$ of myocardium normalized to $\Delta 1/T_1$ of blood and found to be 36.4% (*Figure 1*, Panel D). The patient was transitioned to oral antihypertensives, aspirin, and atorvastatin and was discharged without complication.

Discussion

This case illustrates one of the potential mechanisms for the pathogenesis of HFpEF.[1] Associated medical conditions differ from those associated with HFrEF[3] and include hypertension, hyperlipidaemia, diabetes, chronic lung disease, and obesity, which may contribute to the generation of reaction oxygen species, leading to a pro-inflammatory state. This inflammation may contribute to coronary microvascular dysfunction (CMD) and myocardial fibrosis. Autopsy analysis of 124 hearts of patients with HFpEF demonstrated an inverse relationship between microvascular density and myocardial fibrosis, suggesting that CMD is associated with fibrosis and may contribute to the pathophysiologic mechanism of HFpEF.[4]

Coronary flow reserve and IMR are invasive measurements to measure coronary blood flow[5] and coronary microvascular resistance,[6] respectively. CFR and IMR have been used to determine the presence and severity of CMD in post-cardiac transplant recepients,[7] and to risk-stratify patients with angina without obstructive coronary artery disease.[8] Abnormal CFR and IMR measurements indicate coronary microvascular dysfunction and are associated with poor outcomes.[8] In our patient with HFpEF, CFR was 1.6 (normal >2.5), and IMR 24.5 (normal <20), both abnormal.

Cardiac MRI revealed enlarged left ventricular volumes with normal LVEF, consistent with prior observations in large HFpEF populations.[9] Reduced MPRi can be seen in multivessel obstructive disease but, in the absence of this, may indicate diffuse microvascular dysfunction. The LGE

protocol uses the principle that tissue-specific longitudinal spin-lattice relaxation time (T_1) generates signal contrast between regional myocardial fibrosis and normal myocardium.[10] Infarcted myocardium has undergone scar formation and a much slower washout rate of Gd-based contrast than healthy myocardium and therefore decreased T_1 values detected on LGE imaging. LGE has played important roles in the assessment of ischaemic heart disease as well as other cardiomyopathies. T_1 mapping allows for signal quantification of T_1 relaxation time in milliseconds (ms) per myocardial voxel in order to characterize myocardial tissue. ECV is calculated as the change in the inverse T_1 times in the myocardium normalized to the same in blood, multiplied by estimated water percentage in blood. High ECV has recently been found in HFpEF patients and may correlate with histological extracellular fibrosis and LV stiffness.[11] In addition, an area of focal replacement fibrosis, as indicated by LGE, determines the extent of replacement of myocardium by fibrotic tissue and is a marker for adverse events in ischaemic and non-ischaemic cardiomyopathy. A proposed pathophysiologic mechanism of this phenotype may be described as the development of a systemic inflammatory state in the setting of associated co-morbid conditions in HFpEF including hypertension, chronic kidney disease, and diabetes.[12] Systemic inflammation may lead to reduced nitric oxide (NO) bioavailability.[13] NO activates protein kinase-induced phosphorylation of titin, which is responsible for diastolic recoil and cardiac myocyte distensibility. Reduced NO bioavailability leads to endothelial-dependent microvascular dysfunction with the downstream effect of titin hypophosphorylation and resulting increased diastolic stiffness.[14] Furthermore, systemic inflammation associated with HFpEF comorbidities may lead to transforming growth factor-β conversion of cardiac fibroblast into myofibroblasts, which in turn increases type 1 collagen formation and deposition into the extracellular membrane ultimately causing diastolic stiffness.[15] This potential pathway is far from proven, with further studies needed to better understand the pathophysiologic mechanism of this observed phenotype of HFpEF. This patient exemplifies a potential HFpEF phenotype characterized by CMD, diffuse interstitial and focal fibrosis, which may contribute to diastolic stiffness, elevated filling pressures, and heart failure symptoms.

Conflict of interest

None declared.

Funding

References

1. Steinberg BA, Zhao X, Heidenreich PA, Peterson ED, Bhatt DL, Cannon CP, Hernandez AF, Fonarow GC. Get with the Guidelines Scientific Advisory C, Investigators. Trends in patients hospitalized with heart failure and preserved left ventricular ejection fraction: prevalence, therapies, and outcomes. *Circulation* 2012; **126**: 65–75.

2. Redfield MM. Heart failure with preserved ejection fraction. *N Engl J Med* 2016; **375**: 1868–1877.

3. Ho JE, Enserro D, Brouwers FP, Kizer JR, Shah SJ, Psaty BM, Bartz TM, Santhanakrishnan R, Lee DS, Chan C, Liu K, Blaha MJ, Hillege HL, van der Harst P, van Gilst WH, Kop WJ, Gansevoort RT, Vasan RS, Gardin JM, Levy D, Gottdiener JS, de Boer RA, Larson MG. Predicting heart failure with preserved and reduced ejection fraction: the international collaboration on heart failure subtypes. *Circ Heart Fail* 2016; **9**: pii: e003116.

4. Mohammed SF, Hussain S, Mirzoyev SA, Edwards WD, Maleszewski JJ, Redfield MM. Coronary microvascular rarefaction and myocardial fibrosis in heart failure with preserved ejection fraction. *Circulation* 2015; **131**: 550–559.

5. Baumgart D, Haude M, Liu F, Ge J, Goerge G, Erbel R. Current concepts of coronary flow reserve for clinical decision making during cardiac catheterization. *Am Heart J* 1998; **136**: 136–149.

6. Aarnoudse W, van den Berg P, van de Vosse F, Geven M, Rutten M, Van Turnhout M, Fearon W, de Bruyne B, Pijls N. Myocardial resistance assessed by guidewire-based pressure-temperature measurement: in vitro validation. *Catheter Cardiovasc Interv* 2004; **62**: 56–63.

7. Yang HM, Khush K, Luikart H, Okada K, Lim HS, Kobayashi Y, Honda Y, Yeung AC, Valantine H, Fearon WF. Invasive assessment of coronary physiology predicts late mortality after heart transplantation. *Circulation* 2016; **133**: 1945–1950.

8. Lee JM, Jung JH, Hwang D, Park J, Fan Y, Na SH, Doh JH, Nam CW, Shin ES, Koo BK. Coronary flow reserve and microcirculatory resistance in patients with intermediate coronary stenosis. *J Am Coll Cardiol* 2016; **67**: 1158–1169.

9. Maurer MS, Burkhoff D, Fried LP, Gottdiener J, King DL, Kitzman DW. Ventricular structure and function in hypertensive participants with heart failure and a normal ejection fraction: the Cardiovascular Health Study. *J Am Coll Cardiol* 2007; **49**: 972–981.

10. Stanton T, Leano R, Marwick TH. Prediction of all-cause mortality from global longitudinal speckle strain: comparison with ejection fraction and wall motion scoring. *Circ Cardiovasc Imaging* 2009; **2**: 356–364.

11. Rommel KP, von Roeder M, Latuscynski K, Oberueck C, Blazek S, Fengler K, Besler C, Sandri M, Lucke C, Gutberlet M, Linke A, Schuler G, Lurz P. Extracellular volume fraction for characterization of patients with heart failure and preserved ejection fraction. *J Am Coll Cardiol* 2016; **67**: 1815–1825.

12. Edelmann F, Stahrenberg R, Gelbrich G, Durstewitz K, Angermann CE, Dungen HD, Scheffold T, Zugck C, Maisch B, Regitz-Zagrosek V, Hasenfuss G, Pieske BM, Wachter R. Contribution of comorbidities to functional impairment is higher in heart failure with preserved than with reduced ejection fraction. *Clin Res Cardiol* 2011; **100**: 755–764.

13. Paulus WJ, Tschope C. A novel paradigm for heart failure with preserved ejection fraction: comorbidities drive myocardial dysfunction and remodeling through coronary microvascular endothelial inflammation. *J Am Coll Cardiol* 2013; **62**: 263–271.

14. Borbely A, Falcao-Pires I, van Heerebeek L, Hamdani N, Edes I, Gavina C, Leite-Moreira AF, Bronzwaer JG, Papp Z, van der Velden J, Stienen GJ, Paulus WJ. Hypophosphorylation of the Stiff N2B titin isoform raises cardiomyocyte resting tension in failing human myocardium. *Circ Res* 2009; **104**: 780–786.

15. Westermann D, Lindner D, Kasner M, Zietsch C, Savvatis K, Escher F, von Schlippenbach J, Skurk C, Steendijk P, Riad A, Poller W, Schultheiss HP, Tschope C. Cardiac inflammation contributes to changes in the extracellular matrix in patients with heart failure and normal ejection fraction. *Circ Heart Fail* 2011; **4**: 44–52.